JET–P(98)19

Studies in JET Divertors of Varied Geometry I: Non Seeded Plasma Operation

L D Horton, G C Vlases, P Andrew, V Bhatnagar, A Chankin, S Clement, G D Conway, S Davies, J C M de Haas[1], J K Ehrenberg, G Fishpool, E Gauthier[2], H-Y Guo, P J Harbour, L C Ingesson, H J Jäckel, J Lingertat, A Loarte[3], C G Lowry, C F Maggi, G F Matthews, G M McCracken, R Mohanti, R D Monk, R Reichle[2], E Righi[3], G Saibene, R Sartori, R Simonini, M F Stamp, A Taroni, K Thomsen.

JET Joint Undertaking, Abingdon, Oxfordshire, OX14 3EA,
[1]Present Address: Netherlands Foundation for Research in Astronomy, P.O. Box 2, 7990 AA Dwingeloo, Netherlands.
2 Present Address: Département de Recherches sur la Fusion Contrõlée, Association Euratom-CEA, Centre d'Etudes de Cadarache, F-13108 Saint-Paul-lez-Durance, France.
3 Present Address: The NET Team, Max-Planck Institut für Plasmaphysik, Boltzmannstraße 2, D-85748 Garching bei München, Germany.

Preprint of a Paper to be submitted for publication in Nuclear Fusion

July 1998

STUDIES IN JET DIVERTORS OF VARIED GEOMETRY I: NON SEEDED PLASMA OPERATION

L.D. HORTON, G.C. VLASES, P. ANDREW, V. BHATNAGAR,
A. CHANKIN, S. CLEMENT, G.D. CONWAY, S. DAVIES,
J.C.M. de HAAS*, J.K. EHRENBERG, G. FISHPOOL, E. GAUTHIER†,
H.-Y. GUO, P.J. HARBOUR, L.C. INGESSON, H.J. JÄCKEL,
J. LINGERTAT, A. LOARTE‡, C.G. LOWRY, C.F. MAGGI,
G.F. MATTHEWS, G.M. McCRACKEN, R. MOHANTI, R.D. MONK,
R. REICHLE†, E. RIGHI‡, G. SAIBENE, R. SARTORI,
R. SIMONINI, M.F. STAMP, A. TARONI, K. THOMSEN,
Jet Joint Undertaking
Abingdon, U.K. OX14 3EA

ABSTRACT. Results of experiments investigating the performance of the JET Mark IIA divertor are reported and compared to the performance of its Mark I predecessor. The principal effect of reducing the divertor width (increasing closure) was to increase pumping for both deuterium and impurities while reducing upstream neutral pressure. Neither the orientation of the divertor target relative to the divertor plasma nor the width of the divertor had a major influence on core plasma performance in ELMy H-modes. Changing the core triangularity and thus the edge magnetic shear modifies the ELM frequency in ELMy H-mode plasmas thereby changing the peak divertor power loading. The integrated performance of the core and divertor plasmas is reviewed with a view to extrapolation to the requirements of ITER. The confinement of JET ELMy H-modes with hot, medium density edges is good and follows gyro-Bohm scaling. The impurity content of these discharges is low and within the ITER requirements. When one attempts to raise the density with deuterium gas fuelling the ELM frequency increases and the confinement, especially in the edge, decreases. Good confinement can be achieved in JET either by producing a large edge pedestal, typically in discharges with neutral beam heating or by centrally peaked heating with ICRH schemes. Large amplitude, Type I ELMs, which are present in all discharges with a large edge pedestal, would result in unacceptable divertor plate erosion when scaled to ITER. Since the power deposition profile due to α heating in ITER is calculated to be intermediate between JET NB and RF heating profiles, it is likely that operation in ITER with small ELMs in order to reduce first wall loading will result in degraded confinement compared to present day scaling laws.

1. INTRODUCTION

The JET Mark IIA divertor was installed during a shutdown which was completed in March 1996. Since that time experiments have been performed to characterise the performance of the more closed geometry of Mark IIA as compared to its Mark I predecessor. The poloidal cross sections of the Mark I and Mark IIA divertors are shown in Fig. 1. The magnetic flux expansion in the divertor region can be varied substantially on JET by using the innermost and outermost divertor coils, whilst the X-point height can be adjusted using the lower divertor coil pair, making operation on both horizontal and vertical targets possible in both Mark I and Mark IIA.

For ELMy H-mode discharges on the horizontal targets and standard flux expansion (no current in the outboard coils), the vertical sides of the divertor correspond typically to the 2 cm outer midplane flux surface in Mark IIA, the 3 cm flux surface for the inner divertor leg in Mark I, and the 6 cm flux surface for the outer leg.

The Mark IIA divertor has been operated both with significant leakage paths for neutrals from the divertor pumping plenum into the main chamber and with these leaks reduced by a factor of three [1]. In this paper we will refer to experiments carried out before the reduction of the leaks as being in the MarkIIA divertor and those afterwards, in the "plugged" version, as being in the Mark IIAP divertor. Experiments whose results did not vary with the

*Present Address: Netherlands Foundation for Research in Astronomy, P.O. Box 2, 7990 AA Dwingeloo, Netherlands

†Present Address: Département de Recherches sur la Fusion Contrôlée, Association Euratom-CEA, Centre d'Etudes de Cadarache, F-13108 Saint-Paul-lez-Durance, France

‡Present Address: The NET Team, Max-Planck Institut für Plasmaphysik, Boltzmannstraße 2, D-85748 Garching bei München, Germany

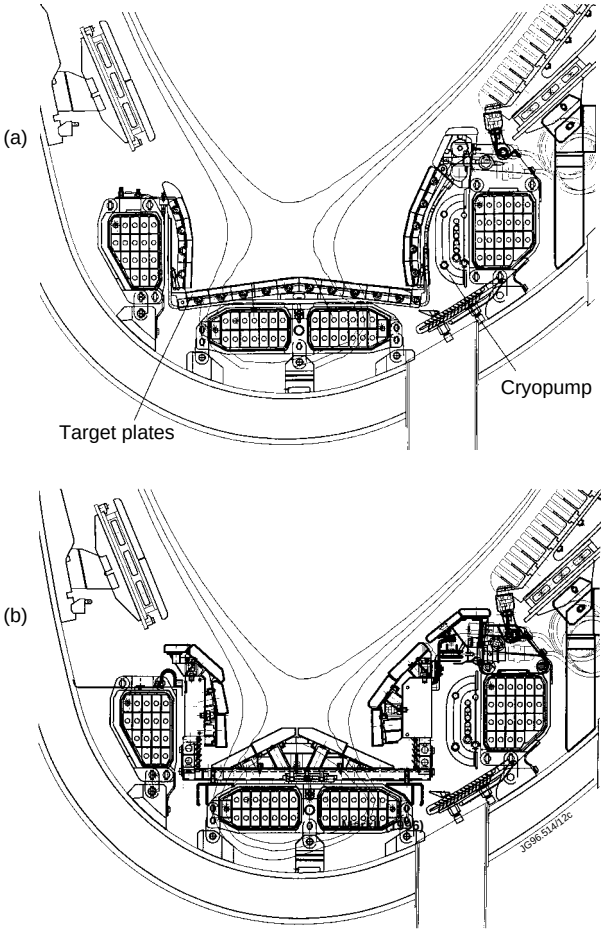

FIG. 1. Poloidal cross sectional view of the JET Mark I (top) and Mark IIA (bottom) divertors.

value of the leaks in the new divertor geometry will be referred to as Mark II. The main goal of these experiments has been to identify an integrated core and divertor plasma operating scenario which meets the needs of next step devices. Two main paths have been followed: operation at high core density using deuterium fuelling alone, while maintaining Type I ELMs; and operation with seeding of an extrinsic impurity to enhance radiation losses and to modify the plasma edge so as to produce Type III ELMs. Here we will report the results of our experiments to investigate the first scenario. The results from the impurity seeded discharges are reported in a companion paper [2].

The term divertor "closure" in this context refers to the degree to which neutrals recycling from the target plates escape from the divertor region. Closure depends on the divertor plasma temperature, density and magnetic geometry as well as on the geometry of the divertor components. In general, a "geometrically closed" divertor will have a larger effect on closure in the low recycling and the detached plasma limits, where the ionisation mean free path becomes large relative to characteristic divertor plasma length scales, as compared to the intermediate high recycling regime.

The reasons for increasing closure are (a) to provide easier access to the regime of high volumetric losses in the divertor, thus reducing target heat loading, (b) to reduce the neutral density in the main chamber, which reduces sputtering of impurities and may improve main plasma confinement quality, and (c) to increase neutral pressure in the divertor chamber, thus facilitating pumping. At the same time, improved closure generally leads to reduced parallel flow in the scrape-off layer (SOL) which results in poorer removal of impurities and ash from the main chamber; this can be partly offset by increased pumping. In general choosing the correct geometrical closure for a divertor is a compromise. One wants to decrease the distance between plasma and divertor structure so as to reduce escape paths for neutrals recycled at the divertor target and while still maintaining sufficient clearance to avoid strong plasma interaction with the structure. In this sense, operation with Type I ELMs is particularly difficult because of the great disparity in effective SOL width between and during ELMs [3].

It is not sufficient to evaluate the performance of different divertor geometries solely on the basis of parameters in the divertor (pumping speed, erosion rates, etc.). The performance of the core plasma must simultaneously be maintained at the levels required for a reactor. The ITER reference point requires a core confinement at the value obtained using the 1997 ELMy H-mode scaling law [4], a core density about 20% greater than the Greenwald value [5] and a core Z_{eff} value of approximately 1.6, excluding helium ash. Considerable emphasis has been placed in the JET divertor programme on studying the compatibility of the various reactor requirements and on mapping the available operating space which can simultaneously be achieved.

2. DIRECT RESULTS OF IMPROVED DIVERTOR CLOSURE

2.1. Access to Detached Regimes

When operating at very low divertor plasma temperatures, either due to high core densities or to large

radiated power fractions, the flux of ions to the divertor target plates is seen to be dramatically reduced from what one would expect from a simple high recycling divertor model where the ion flux increases with the square of the upstream (separatrix) density. This phenomenon is commonly referred to as divertor detachment. Operating in a detached regime significantly reduces peak heat loading and physical sputtering of the divertor and is thus potentially an important benefit to a fusion reactor in which the lifetime of divertor components can have a strong impact on the overall cost of electricity.

To allow the quantitative comparison of detachment experiments, a new method of evaluating the degree and operating window of detachment has been introduced using the ion flux measurements at the divertor target [6]. In this definition the degree of detachment (DOD) is defined as the inverse ratio of the measured ion flux to that which one would expect in a high recycling divertor:

$$DOD = \frac{I_d^{scal}}{I_d^{measured}} \tag{1}$$

and

$$I_d^{scal} = C \cdot \overline{n}_e^2 \tag{2}$$

where $\overline{n}_e$ is the core plasma line-averaged density and the proportionality constant, C, is obtained experimentally from the low density phase of the discharge where the DOD is assumed to be one. In Fig. 2, the degree of detachment is plotted as function of the core density for L-mode discharges in Mark I and Mark IIA. Defining the onset of detachment as being the density at which $DOD = 2$, one finds that in the Mark IIA divertor the onset of detachment is reduced by approximately 30% relative to Mark I. Furthermore, the approach to the density limit following the onset of detachment is much more abrupt in Mark IIA, relative to Mark I.

During ELMy H-modes with D_2 fuelling it is possible to obtain plasma detachment in between but not during the ELM events. The degree of detachment in ELMy H-mode discharges is difficult to determine because of the perturbations introduced by the ELMs, because the separatrix density is probably not proportional to the line-averaged density (unlike L-modes), and because of the narrow density range accessible, especially in neutral beam-heated shots. Nevertheless, the variation of the ion saturation current during the density rise immediately after the H-mode transition suggests that the degree of detachment of our ELMy H-modes is only about two as

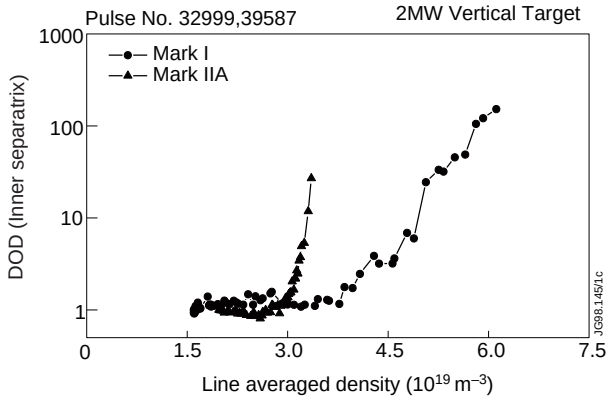

FIG. 2. Degree of detachment of the inner divertor separatrix as a function of core plasma line-averaged density for two vertical target L-mode discharges, one in the Mark I and one in the Mark IIA divertor.

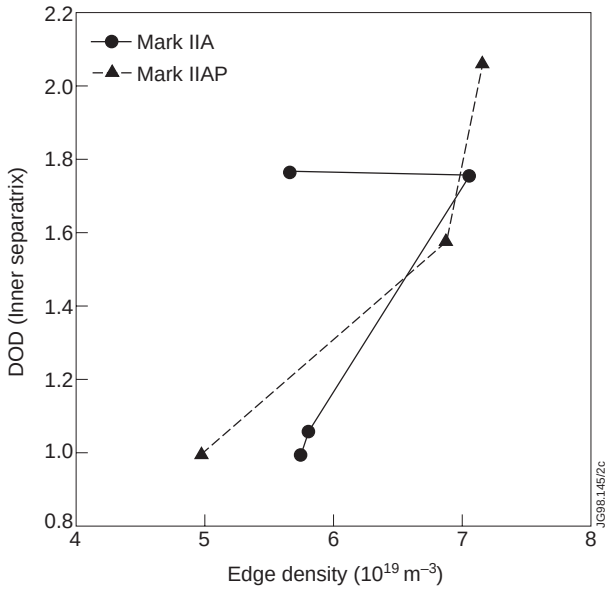

FIG. 3. The degree of inner divertor separatrix detachment as a function of edge plasma density for two series of ELMy H-mode discharges, one from Mark IIA and one from Mark IIAP. Discharges in each series are at 2.5 MA, 2.5 T with 12 MW of neutral beam heating and differ by the amount of deuterium gas fuelling provided in addition to the neutral beam fuelling.

compared to an upper limit of close to one hundred in L-mode discharges (Fig. 3). These measurements of low divertor detachment in ELMy H-modes are confirmed by simulations using the EDGE2D/U edge transport code [7].

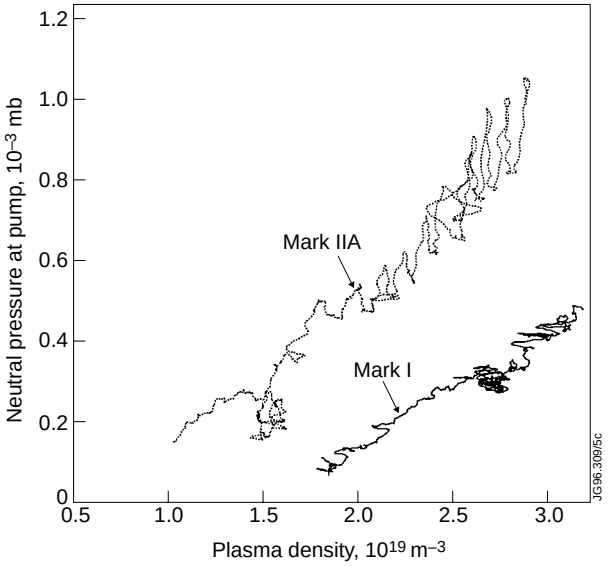

FIG. 4. Comparison of subdivertor pressures (and thus of deuterium pumping speeds) for Ohmic pulses in the Mark I and Mark IIA divertors.

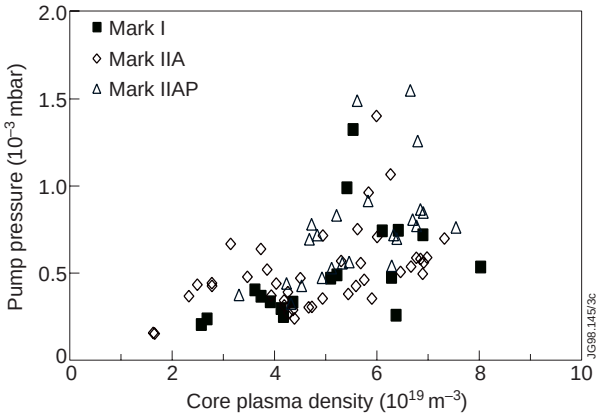

FIG. 5. The pressure measured next to the divertor cryopump as a function of line-averaged core plasma density for ELMy H-modes in the different JET divertor geometries. Only discharges with good confinement ($H_{97} > 0.9$) and similar triangularities ($0.175 < \delta < 0.225$) are included.

2.2. Pumping

One of the most notable consequences of increasing the divertor closure was to increase the pumping both of deuterium and of recycling impurities. In going from Mark I to Mark IIA the neutral pressure next to the divertor cryopump (and thus the deuterium pumping speed) increased by a factor of two to three in L-mode discharges (Fig. 4). This factor of two to three increase in pumping speed was predicted by EDGE2D/U modelling in which only the divertor geometry was varied.

In contrast to Ohmic and L-mode discharges, in ELMy H-mode discharges the pumping speed for a given core line-averaged density did not increase with divertor closure (Fig. 5). In steady state the exhaust rate must be equal to the fuelling rate and the plasma separatrix density, which is the density that controls the divertor density and thus the exhaust rate, will adjust in such a way so as to achieve this balance. In ELMy H-modes, as opposed to L-mode discharges, it is known that the ratio of the separatrix density to the core density varies with gas fuelling rate (see Section 3.4). There being no direct comparisons of separatrix densities between Mark I and Mark II in JET, it is impossible to conclude whether or not pumping in Mark II in ELMy H-modes has improved for a given separatrix density.

When comparing Mark I with Mark II there are two competing effects which will determine whether the separatrix density must be higher or lower for a given fuelling rate. In the more closed geometry of Mark II one would expect neutrals which are recycled at the divertor target plates to be more efficiently pumped as is seen in the L-mode data. Thus, in steady state, the separatrix density must adjust itself so as to provide particle balance. On the other hand, in the more closed geometries a greater fraction of the neutrals produced by ELMs is located on the entrance baffles above the divertor rather than on the target plates. Since only neutrals which are recycled inside the divertor are likely to be pumped, the separatrix and divertor density must rise.

In order to study impurity exhaust, a series of dedicated experiments was performed in L-mode discharges using neon as a trace, recycling impurity. In these experiments a small quantity of neon was puffed into the SOL, introducing an initial neon concentration in the core plasma which then decayed with an e-folding time, τ_{Ne}. In all three divertor geometries this decay time was very long without the cryopump activated, indicating that neon is a fully recycling impurity. When the pump was used, τ_{Ne} varied from 3-5 s in Mark I to around 1 s in Mark IIA and IIAP (Fig. 6). In all three series of experiments τ_{Ne} decreased by a factor of two with increasing plasma density over the range accessible in L-mode plasmas. The neon exhaust rates for Mark IIA and Mark IIAP are indistinguishable when the decay time is plotted as a function of divertor plenum pressure or, equivalently, of deuterium exhaust rate. In this way it can be seen that the neon exhaust rate is proportional to the deuterium exhaust rate from the divertor, at least for a given divertor geometry.

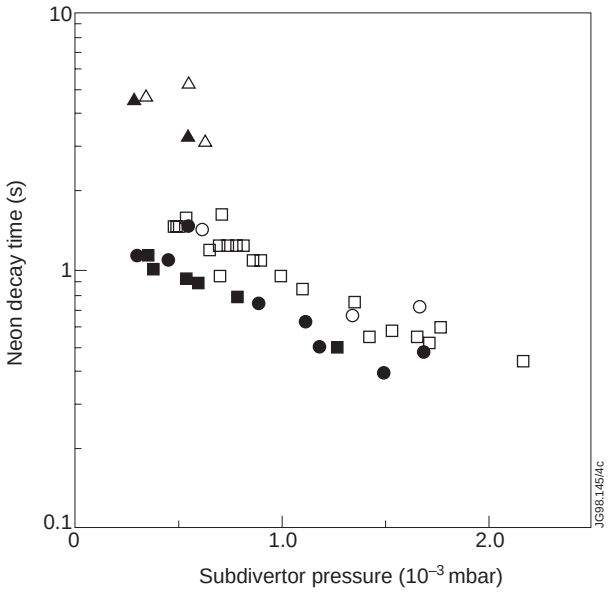

FIG. 6. The decay time of neon emission after the neon source is removed as a function of the pressure in the subdivertor volume next to the divertor cryopump. Data are plotted separately for Mark I (triangles), Mark IIA (circles) and Mark IIAP (squares) divertors. Solid points correspond to cases where the deuterium fuelling is from the top of the main chamber and the open points to cases where the deuterium fuelling was into the divertor. All discharges were L-modes with an input power of 3 MW.

One of the aims of the series of neon experiments was to investigate the influence of controlled convection on the retention of neon in the divertor. This was done by changing the position of the deuterium fuelling between the top of the machine and the divertor. Once the influence of the deuterium exhaust rate is recognised, it is possible to see the improved neon exhaust resulting from top fuelling (Fig. 6). While an indirect cause, such as changes in the SOL parameters depending on the location of the fuelling cannot be ruled out, this is strong evidence that convection is improving the exhaust of impurities in JET.

2.3. Neutral Compression

Increasing the divertor closure has led to an increase in the neutral compression in the subdivertor volume (Fig. 7). This compression has been measured in two ways: (a) using the ratio of the subdivertor pressure measured next to the divertor cryopump to the D_α signal measured along a horizontal chord through the centre of the plasma; and (b) using the ratio of the subdivertor pressure to the neutral pressure measured at the outer midplane of the vacuum vessel. The $D\alpha$ light is known by Zeeman splitting

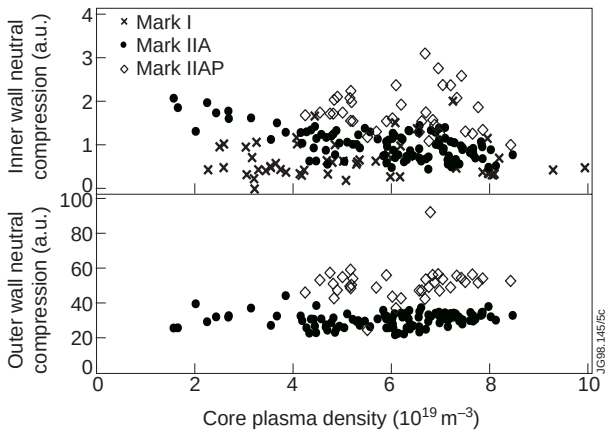

FIG. 7. Two methods of measuring the neutral compression into the subdivertor volume: (a) The ratio of the subdivertor pressure measured next to the divertor cryopump to the $D\alpha$ light measured along a horizontal chord through the centre of the plasma; and (b) the ratio of the subdivertor pressure to the outer midplane pressure, both plotted as a function of line-averaged core electron density.

measurements to come primarily from the inner edge of the core plasma and the ratio is thus a measure of the compression along the inner SOL. Unfortunately, calibrated midplane pressure measurements are not available for Mark I. Nevertheless, the trend towards improved compression with divertor closure is clear.

2.4. Core Plasma Impurity Content

The impurity content, as measured by charge exchange spectroscopy for carbon and by X-ray crystal spectroscopy for nickel, of high density Mark IIA and Mark IIAP ELMy H-mode discharges is similar to that in Mark I (Fig. 8). This is despite the fact that reduced neutral pressure in the main chamber should lead to lower levels of sputtering in the region where impurities most efficiently contaminate the core. One explanation is that ion impact on components forming the narrow entrance of the closed Mark II divertor, especially during ELMs, is the dominant source of impurities at high density. A second possibility is that the chemical sputtering in Mark IIA is higher than in Mark I due to higher tile temperatures in the non-wetted areas of the divertor, an effect which is unrelated to closure. A third possible cause is the cladding of the inner wall with carbon tiles which took place at the time of the plugging of the bypass leaks (MarkIIA $\rightarrow$ IIAP).

The intrinsic impurity concentrations in the plasma core and impurity influxes have been stud-

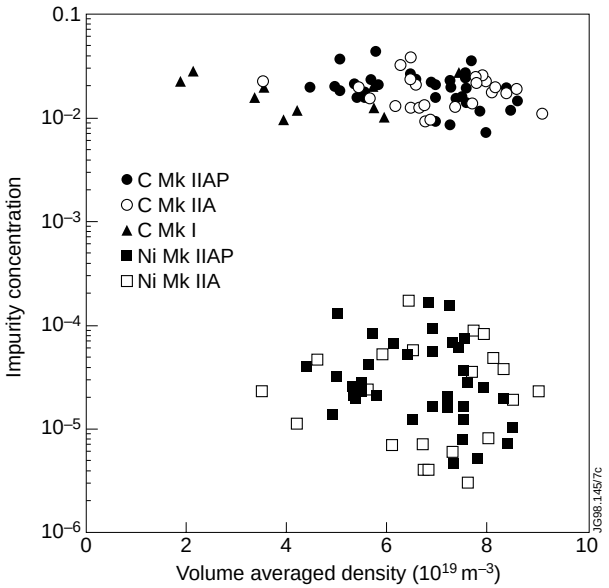

FIG. 8. Concentrations of carbon and nickel in the core plasma of ELMy H-mode discharges for the various JET divertors as a function of volume-averaged density.

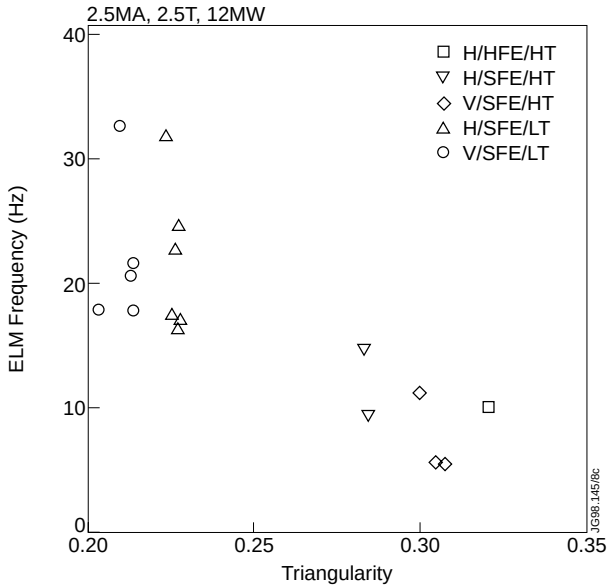

FIG. 9. ELM frequency versus triangularity for Mark IIA pulses with beam fuelling only. The designation of the equilibria A/BBB/CC indicates target orientation (horizontal or vertical), flux expansion (high or standard), and triangularity (high or low), respectively. All of the pulses were run at 2.5MA, 2.5T, and with 12MW of NB power.

ied in detail as a function of divertor closure, both for the different divertor geometries and by varying the magnetic geometry. The results of these studies are reported in a companion paper [8].

3. STUDIES OF STEADY STATE ELMY H-MODES

The ELMy H-mode is the preferred operating scenario for ITER. Studying the compatibility of ELMy H-modes with closed divertor configurations, especially in regimes of partial and complete detachment, was one of the main goals of the JET Mark II divertor programme. It can be shown that it is impossible in existing experiments to simultaneously match the dimensionless plasma parameters of ITER in the core and the divertor plasmas [9]. This means that a true similarity experiment cannot be done and that it is necessary to obtain an understanding of how the local transport is linked between the core and the divertor in order to make predictions of performance of next generation devices. It is for this reason that research in the divertor field is moving more and more towards local analysis rather than simply using global parameters as figures-of-merit.

3.1. Influence of Magnetic Configuration

In order to isolate the effects arising from configurational changes, a series of Mark IIA discharges was carried out with fixed plasma current, magnetic field, and neutral beam power (2.5 MA, 2.5 T, and 12 MW, respectively), in which the target orientation (horizontal or vertical targets), flux expansion (horizontal target only), and main plasma triangularity were varied. It was found that these discharges reached nearly steady state conditions within about 3 seconds of applying the beam power and that this state was characterised by regularly spaced Type I ELMs. In the absence of gas puffing, the ELM frequency, f_E, depends most strongly on triangularity, without reproducible dependencies on target orientation or flux expansion, as shown in Fig. 9.

The confinement of the discharges in these scans, with and without gas fuelling in addition to beam fuelling, is shown in Fig. 10. For a given input power, plasma current, and toroidal field, the stored energy in the plasma does not depend strongly on magnetic configuration (Fig. 10(a)). When normalised to the 1997 scaling law (H_{97}), however, the low triangularity pulses outperform those at high triangularity (Fig. 10(b)), both at a given ELM frequency and at the lowest ELM frequency which is accessible for a given configuration, i.e. with beam-fuelling only and a well conditioned vacuum vessel. This is because the JET data do not follow the density dependence in the scaling law; when the confinement is repre-

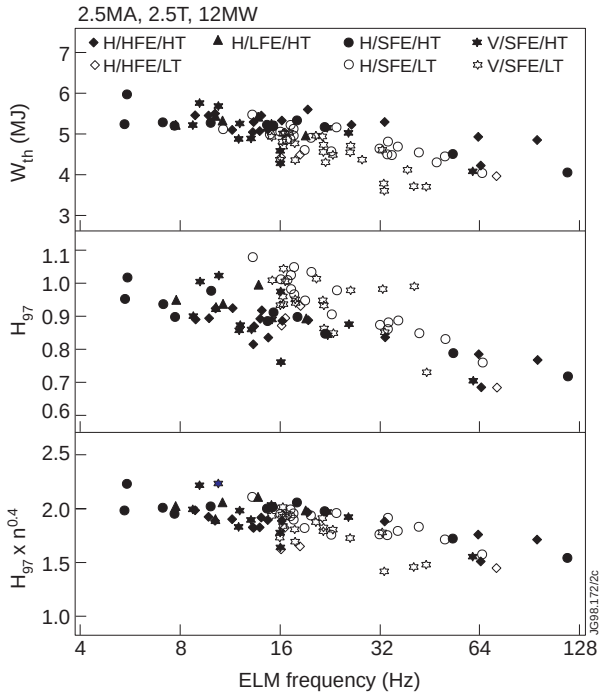

FIG. 10. Dependence of confinement on ELM frequency for beam-heated pulses in Mark II at 2.5 MA and 2.5 T with 12 MW of heating power: (a) the plasma thermal stored energy, (b) the energy confinement time normalised to the 1997 ELMy H-mode scaling law (H_{97}), and (c) H_{97} with its density dependence removed.

sented by removing the density dependence from H_{97} (Fig. 10(c)) there is little remaining dependence on configuration other than through ELM frequency. In all the configurations tested the global confinement degrades with increasing ELM frequency.

The density of beam-fuelled only discharges decreases with increasing ELM frequency. Z_{eff} also drops as f_E increases, suggesting that either small ELMs produce fewer impurities or that the more frequent ELMs are more effective at purging the edge plasma of impurities (see also [8]). The total radiated power fraction in these discharges was quite low for the high ELM frequency configurations, around 25%, increasing at lower ELM frequencies to about 40%.

3.2. H-mode Density Limit and Degradation of τ_E

To reach ignition, ITER needs to operate in a high confinement regime with low Z_{eff} and at a plasma density of about 1.2 times the Greenwald density limit (GDL). Experiments were therefore carried out in the JET Mark IIA and Mark IIAP campaigns to determine the maximum density compatible with $H_{97} > 0.9$ in steady state, partially detached discharges.

In a similar series of discharges to those described above, the deuterium fuelling rate was systematically varied in strength and location [10]. The ELM frequency was found to increase with the addition of heavy gas fuelling. For moderate gas fuelling rates ($< 2\times10^{22}$atoms/s) there is a small rise in the core density (Fig. 11). With the increase in ELM frequency, the electron pressure at top of the transport barrier at the plasma edge, averaged over the ELM cycles, decreases [11]. In some cases, especially when comparing beam-fuelled pulses with those with additional gas fuelling, there is an increase in the core confinement which compensates for the degradation at the edge, leaving the total stored energy approximately constant. Because of the density dependence in the 1997 ELMy H-mode scaling law, H_{97} decreases in this range of fuelling, even when there is no decrease in the stored energy. With increasing gas puffing the edge particle and energy confinement quality continue to decline, so that there is a maximum density which can be obtained before the confinement degradation outweighs the increased puffing and the fuelling efficiency becomes effectively negative. At the levels of gas fuelling where the density drops, the global confinement, whether measured by the plasma stored energy or relative to H_{97}, is significantly degraded (Fig. 11). The highest densities were achieved in more triangular plasmas but at the expense of reduced ELM frequency, higher peak divertor load and higher impurity content [8]. Little difference was found in either confinement or attainable density between horizontal and vertical target discharges.

Experiments were also performed to raise the core density using shallow pellet fuelling ($v < 600$m/s) [12]. At the penetration available with the present injector it is not possible to raise the density of an ELMy H-mode; each pellet is followed immediately by an ELM which expels the injected material. While this is disappointing from the point of view of plasma fuelling, it does provide a potential mechanism for control of ELM frequency and thus of peak divertor power loads.

The maximum density achieved in steady state conditions with $H_{97} > 0.9$ is 0.8 GDL. We introduce a figure of merit:

$$\frac{H_{97}\cdot\overline{n}_e}{n_{GDL}} = \frac{\overline{n}_e\cdot\tau_E}{n_{GDL}\cdot\tau_{ITER97}}, \qquad (3)$$

which measures the confinement-density product relative to that required by ITER. This is shown in

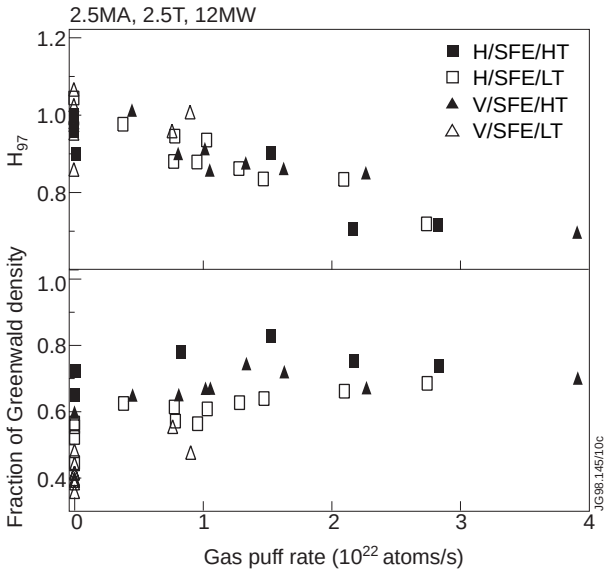

FIG. 11. (a) Confinement enhancement relative to the 1997 ELMy H-mode confinement scaling law (H97) as a function of deuterium gas fuelling in the various MarkIIA configurations. (b) Plasma density achieved (as a fraction of the Greenwald limit) against deuterium gas fuelling for the discharges in (a).

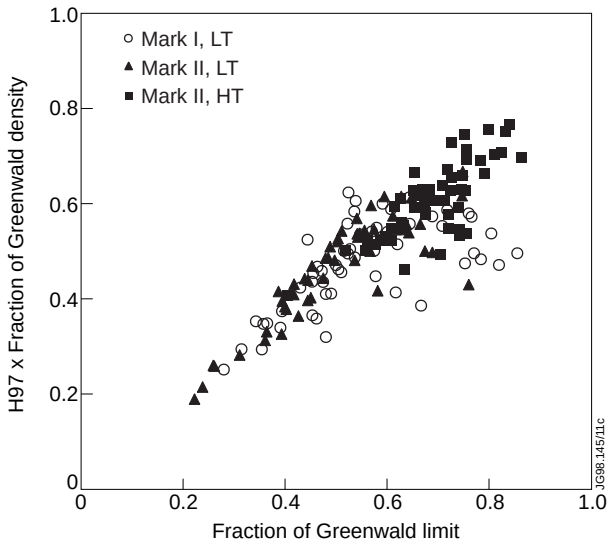

FIG. 12. The product of the core plasma confinement, normalised to the 1997 ELMy H-mode scaling law, and the core density, normalised to the Greenwald limit, versus the normalised density. The circles are Mark I discharges which were all with low triangularity, the triangles are Mark II low triangularity discharges, and the squares are Mark II high triangularity shots.

Fig. 12 for Mark I and Mark II. The best performance is at high triangularity ($0.26 < \delta < 0.33$). At lower triangularity there is little difference between Mark I and Mark II. As observed in other machines, the maximum density is independent of input power and scales slightly less than linearly with plasma current, in approximate agreement with the Greenwald formulation. There is no difference in the attainable confinement-density product between Mark IIA and Mark IIAP.

3.3. Analysis of Confinement Degradation

It is instructive to see where one of the ELMy H-mode gas scans lies in the edge operating diagram [13]. In JET, measurements of the electron temperature at the top of the edge pedestal are available from the ECE heterodyne radiometer. The density at the top of the pedestal is estimated by the line-averaged density measured on a vertical chord at a major radius of 3.75 m by the far-infrared interferometer. Since the outer mid-plane separatrix is located at about 3.8 m and the density profile is generally quite flat inside the pedestal, this density is thought to be close to the density at the top of the edge pedestal. The data for a gas scan in a series of discharges on the vertical divertor target plates is shown in Fig. 13. As gas is added to the discharge the peak edge density (at the ELM) rises and the peak edge temperature falls in such a way that the peak edge electron pressure remains approximately constant [14]. In this range of gas fuelling the pedestal density increases by a factor of two while the core density increases by only 20% (see Fig. 11). Because the edge pressure tends to rise quickly after an ELM and then approach the pressure limit more slowly, the edge pressure averaged over the ELM cycle decreases with increasing ELM frequency [11]. The edge confinement is thus a monotonically decreasing function of ELM frequency. At very high gas rates, where the global confinement has become significantly degraded, the peak edge electron pressure deviates significantly from the curve of approximately constant pressure.

3.4. Dependence on Midplane Pressure and Separatrix Density

Several divertor tokamaks have reported a correlation between degraded H-mode confinement and increasing main chamber neutral pressure [15, 16], and the ITER Team has postulated that the very low main chamber neutral pressure they expect to achieve as a result of their deeply baffled divertor may improve confinement, particularly as detached divertor conditions are approached [17]. In a diverted tokamak with good main chamber wall clearance,

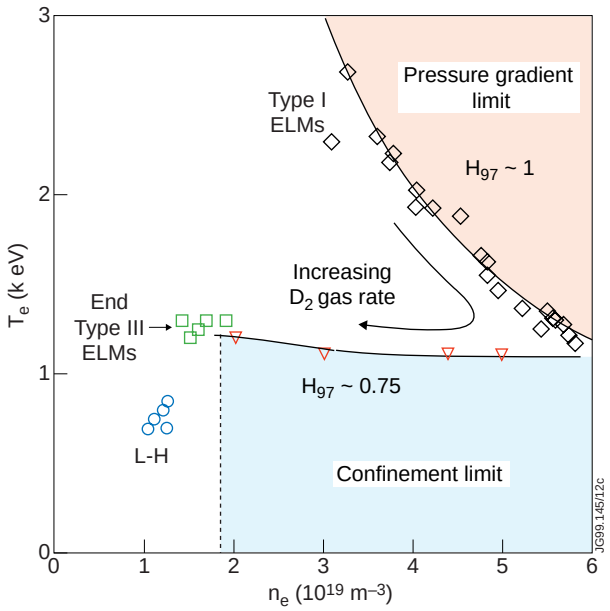

FIG. 13. Plot of edge electron temperature versus edge electron density for a series of vertical target ELMy H-modes with varying rates of gas fuelling. The temperature and density values are representative of values at the top of the edge pedestal taken just prior to an ELM. Typical values for the global confinement factor are also shown.

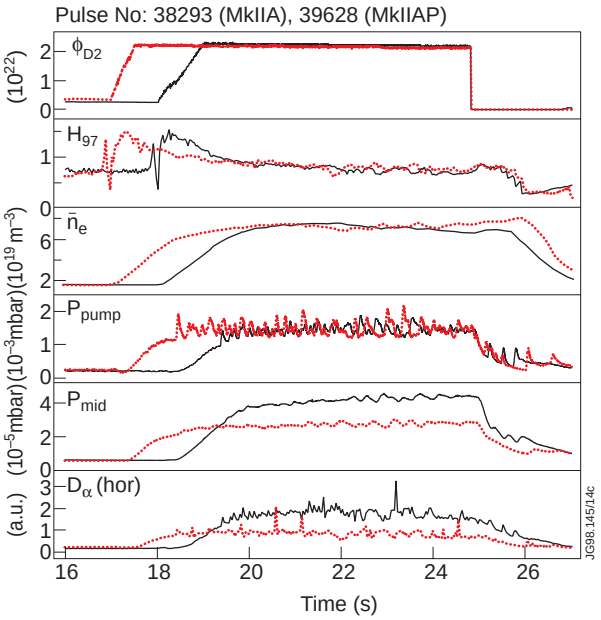

FIG. 14. Time traces of two identical pulses, one before (solid curves) and one after (dashed curves) the reduction of the neutral leakage from the subdivertor volume into the main plasma chamber. Data shown are the gas injection rate, the plasma confinement (H_{97}), the core plasma line-averaged density, the subdivertor neutral pressure, the outer midplane neutral pressure, and the $D\alpha$ emission from a chord which views the plasma horizontally through its midplane.

the primary source of main chamber neutrals is outflux of neutrals, either through the divertor throat or through bypass leaks, which are created at the target plates (CX processes in the main chamber do not create new neutrals). For given divertor/edge plasma conditions and fixed geometry, there is thus a direct correlation between main chamber neutral pressure at the outer midplane ($p_{o,mc}$) and divertor neutral pressure ($p_{o,div}$). Moreover, there is a direct correspondence between miplane separatrix density (n_s), divertor plasma density (n_d), and divertor neutral pressure, so that the causality between confinement factor (H_{97}) and the quantities n_s, $p_{o,mc}$, and $p_{o,div}$ cannot be established in a single geometry experiment.

If the divertor geometry is varied, however, holding plasma conditions fixed, it is in principle possible to prove or disprove causality between H_{97} and $p_{o,mc}$. Such an experiment was carried out in JET when the bypass leaks were reduced by about 75% when going from Mark IIA to Mark IIAP. Identical ELMy H-mode gas scans (2.5 T/2.5 MA/12 MW) were conducted in fixed magnetic configuration before and after the reduction of the leaks. Figure 14 shows time traces for a pair of pulses on the horizontal target with standard flux expansion and high triangularity (H/SFE/HT) and with identical gas fuelling. It can be seen that the two pulses have virtually identical confinement, density and divertor pressure. However, the main chamber neutral pressure ($p_{o,mc}$) for the Mark IIAP pulse is about 35% less than the Mark IIA pulse. Similar results are seen when the inner wall $D\alpha$ signal is used to represent the main chamber pressure.

In Fig. 15 H_{97} is plotted versus subdivertor neutral pressure, midplane pressure, horizontal $D\alpha$, and midplane separatrix electron density for ELMy H-modes from Mark IIA and Mark IIAP. The confinement is strongly correlated to the divertor pressure and to the separatrix density, independent of the divertor geometry, reflecting the fact that $p_{o,div}$ and n_s are strongly correlated. On the other hand, there is a significant reduction of main chamber neutral pressure, for a given core confinement, in the Mark IIAP scans as compared to Mark IIA. This suggests that it is separatrix plasma density rather than the increased main chamber neutral pressure which produces the confinement degradation. Thus these experiments suggest that an increase of confinement quality in ITER

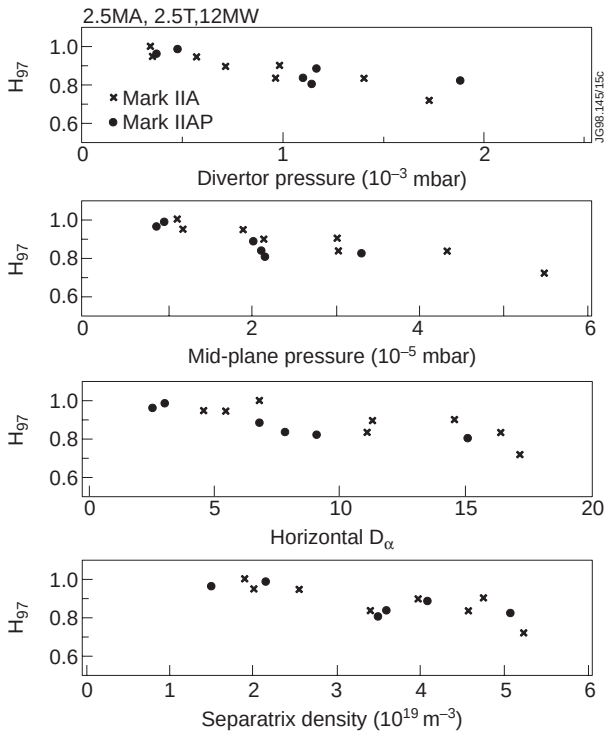

FIG. 15. Variation of the core confinement (H_{97}) with (a) divertor neutral pressure, (b) midplane neutral pressure, (c) horizontal $D\alpha$ emission, and (d) separatrix electron density at the outer midplane.

resulting from reduced main chamber neutral pressure, relative to today's experiments, is unlikely.

3.5. H-mode Threshold

The minimum power required in order to obtain and maintain H-mode levels of confinement is of crucial interest to ITER. Present predictions [18–20] are uncertain to the extent that ITER may or may not operate with improved confinement with α heating alone and thus may or may not ignite.

The various divertor geometries in JET have allowed us to study the influence of divertor closure on the H-mode threshold. This is particularly interesting given the large difference in H-mode threshold found in ASDEX with and without large bypasses connecting the main chamber and the divertor [21]. In contrast, the H-mode threshold in JET does not appear to depend on divertor closure [22]. The threshold for Mark IIA and for Mark IIAP appears to be identical to that found in Mark I (Fig. 16). Similarly, discharges with the divertor strike points on the vertical target plates are predicted to be more closed than those on the horizontal plates (where we have the bulk of our data) but the difference between the

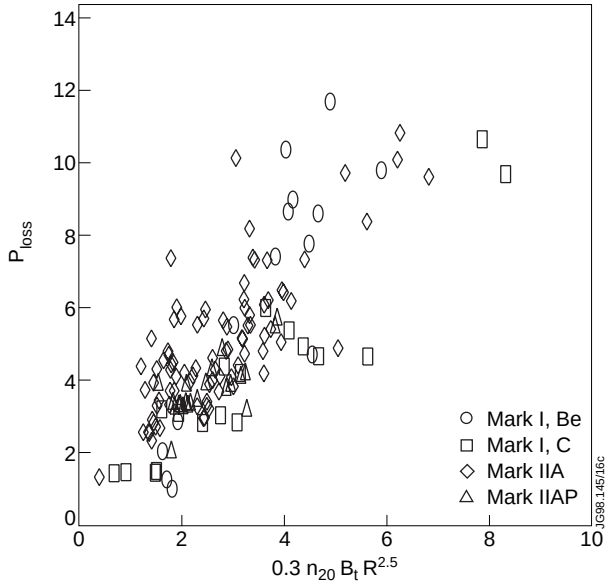

FIG. 16. Threshold power necessary for producing an H-mode in the different JET divertors.

threshold in these two configurations is also small.

3.6. Power and Energy Load on First Wall Components

From a technical standpoint, the "carbon bloom" was completely eliminated in both Mark I and Mark II by shadowing of tile edges and careful alignment [23]. The use of large area tiles in Mark II allowed smaller angle of incidence, giving larger effective target area.

The present ITER design foresees the use of carbon fibre composite (CFC) materials for the divertor strike point region. The predicted lifetime of these components depends on the erosion due to sputtering in normal operation, due to disruptions and due to slow, high power transients [24]. The nominal peak power load to the divertor is $5\,\mathrm{MW/m^2}$ although operation up to $10\,\mathrm{MW/m^2}$ is also possible with component lifetimes of several thousand pulses. In addition to these limits, strong evaporation due to frequent ELMs must be avoided. The ITER team quote $1.2\,\mathrm{MJ/m^2}$ if the ELM duration is 1 ms and $0.45\,\mathrm{MJ/m^2}$ for $100\,\mu$s duration as an upper limit for energy deposition by an ELM [25].

The major difficulty with standard ELMy H-mode operation produced by neutral beam injection is the presence of large amplitude Type I ELMs which deposit high power levels repetitively onto the divertor components. Statistical analysis has been performed for the step changes in the diamagnetic energy

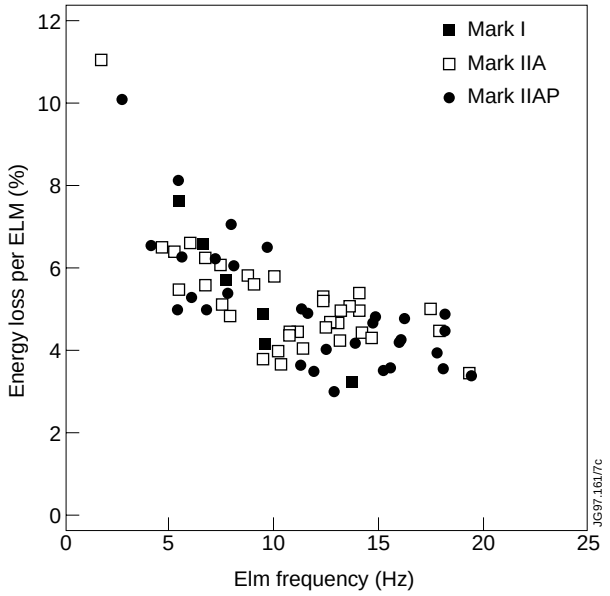

FIG. 17. Percentage of the plasma stored energy lost during an ELM as a function of ELM frequency.

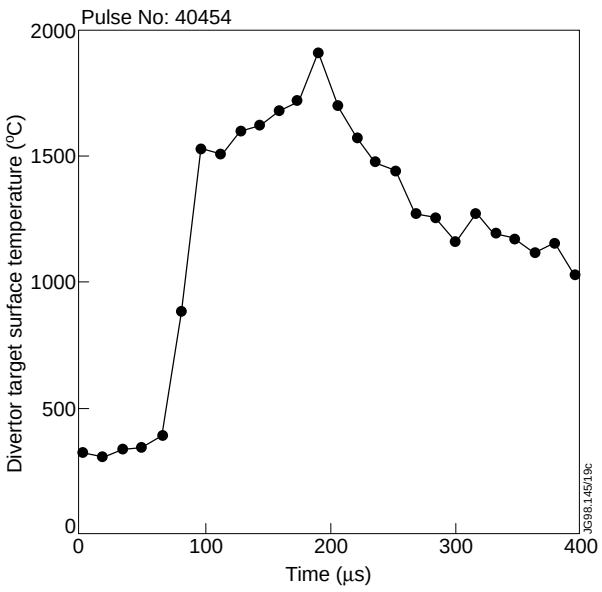

FIG. 18. Time history, in a neutral beam heated discharge, of the divertor target temperature during an ELM at the point of maximum power deposition.

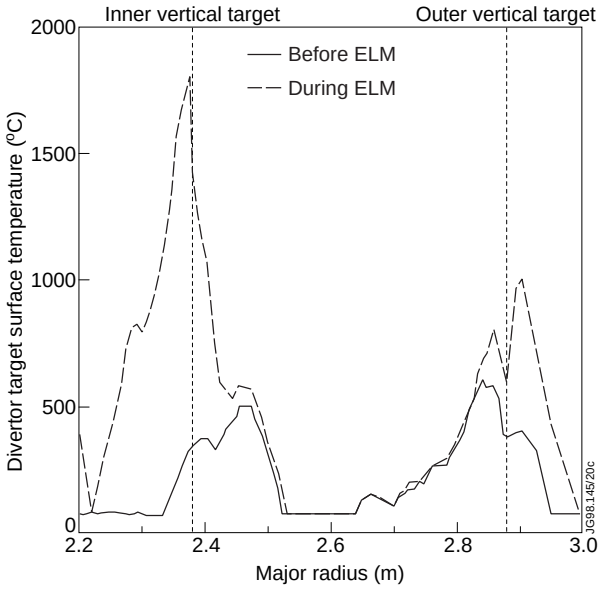

FIG. 19. Profiles of divertor target surface temperature before and during the ELM shown in Fig. 18.

and core density which occur due to ELMs [26]. The results indicate that the percentage change in energy and density decreases approximately as the square root of the ELM frequency (Fig. 17). How this translates into surface heating of the divertor tiles depends on the duration of the heat pulse, the area of interaction, and how much of the ELM energy is radiated. The dynamics of surface power deposition by Type I ELMs are crucial for extrapolation to ITER.

For the first time on JET, direct, high time resolution (13 μs) measurements of the power flux to the divertor during an ELM have been obtained using a fast 2D infrared camera, working in the $3-5\,\mu$m range [27]. The duration of the peak power deposition for typical Type I ELMs is about $120\pm20\,\mu$s and peak temperatures in excess of 1000° C are routinely observed (Fig. 18). Fast interferometer measurements show that particles are lost on a much longer time scale of 3 to 4ms.

During a Type I ELM a fast displacement of the plasma occurs, with the strike zones moving from their initial positions with characteristic times of less than 20 μs. For typical Type I ELMs the peak power deposition occurs at the inner divertor (Fig. 19). This is where the largest motion of the strike points is observed but the movement does not spread uniformly the heat load due to the relative timing of the movement and the power deposition [28]. During an ELM the peak power flux to the inner strike zone is first shifted, typically by about 20 cm to a smaller major radius. The strike zone then moves around this new position inwards or outwards by about 5 cm during the next 120 μs, where the largest power deposition takes place. Data from fast, unfiltered soft X-ray diodes, which act as bolometers, show that radiative losses follow the time of peak power deposition and hence do not significantly reduce the erosion problem.

The temperature histories measured by the IR camera during ELMs are believed to overestimate the actual situation due to the presence of deposited

layers on the tiles with different (unknown) thermal properties. It is thus more appropriate to use the time history and footprint of the power deposition as measured with the IR camera and the plasma energy loss from fast magnetic measurements in order to make an estimate of the peak power and energy density deposited during ELMs in JET. The estimate will, of course, be an upper limit since the fraction of the ELM power which is deposited outside the divertor is not known. In fact, wide angle camera views of the JET vacuum vessel show strong interaction around the torus during ELMs, so a significant fraction of the ELM energy may well be deposited outside the divertor. For a typical JET discharge at 2.5 MA and 2.5 T with 12 MW of NB heating one calculates a peak energy flux of approximately $0.2\,\mathrm{MJ/m^2}$, deposited in about $100\,\mu$s. If this energy was to scale with the plasma stored energy, the energy loss per ELM in ITER would be $35\,\mathrm{MJ/m^2}$, enough to cause strong evaporation of the divertor target.

The measured time dependence of the power and particle deposition during an ELM is consistent with that obtained by 1-D modelling of the SOL response to an ELM [29]. Such 1-D modelling cannot treat the problem of the ELM footprint and thus provides no direct estimate of the peak target loads. New modelling results show that the ELM duration should have a very weak scaling with machine size.

The ELM behaviour of discharges heated with ICRH rather than NB power is typically significantly different (Fig. 20). ELMs in RF H-modes are smaller in amplitude and more frequent. In both the RF and NB-heated discharges the global confinement is good with $H_{97} \approx 1$. The pressure at the edge pedestal is considerably smaller in the RF pulses, however. This is compensated by higher central pressure due to the more central power deposition by RF. Indeed, transport analysis indicates that the core energy transport is the same, independent of the heating method.

In some RF heated discharges large ELMs are observed, either at very high input powers or following a sawtooth crash which temporarily provides high power to the edge plasma. In these cases large, well spaced ELMs are observed and the edge pressure increases to the values typical of neutral beam heated pulses. We thus conclude that one can only obtain large edge pedestal pressures at the price of large ELMs.

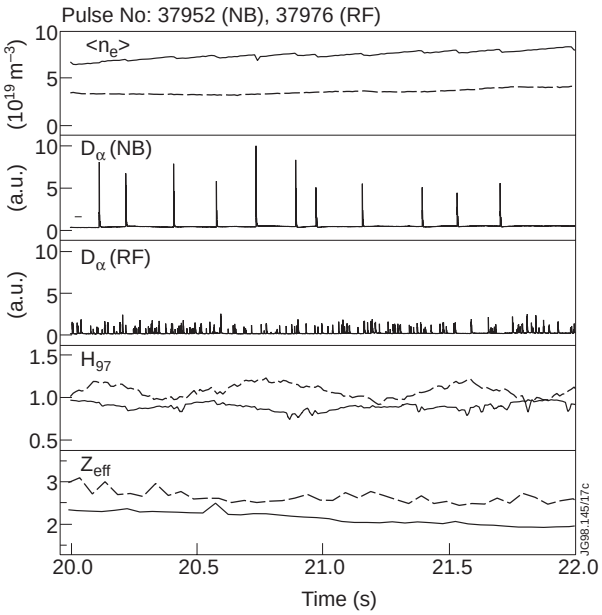

FIG. 20. Example of comparable ELMy H-mode pulses (11 MW, 2.5 MA, 2.5 T) produced by neutral beam heating (solid curves) and radio frequency heating (dashed curves) illustrating the changed character of the ELMs ("D_α" signal).

3.7. High Performance Steady State Operation

The JET tokamak, due to its large size, single null configuration and available range of triangularities, is in a position to produce plasmas which most closely resemble those required for ITER. In JET, as is likely to be the case in ITER, the maximum confinement and fusion performance is found at the highest accessible currents ($I_p \leq$5MA). This is achieved at the expense of operating at values of q_{95} less than three. Above a value of approximately 2.4 we observe no degradation of confinement with q_{95}. If this is found to be true in ITER as well, operation at low q would provide a significantly increased ignition margin.

The highest stored energies and equivalent Q_{DT} values are achieved at the highest plasma current but with a confinement somewhat lower than the prediction of the 1997 ELMy H-mode confinement scaling [30]. In fact, whilst at 2.5MA H_{97}≈1.0, at 4MA H_{97}≈0.9 and above 4MA H_{97}≈0.85. In deuterium plasmas, steady state equivalent fusion power of approximately 4MW has been achieved at 4.7MA with 17MW of NB power and at 3.5MA with 24MW of combined heating (16MW NB + 8MW of ICRH). These results have recently been confirmed in DT plasmas and will be reported elsewhere.

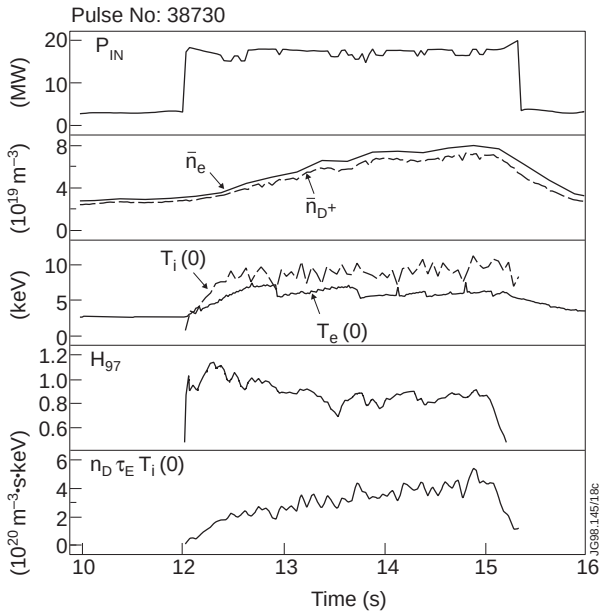

FIG. 21. Time traces of a high power 4.7MA discharge where the fusion triple product reaches a value of $4 \times 10^{20}\mathrm{m}^{-3}\mathrm{s\,keV}$.

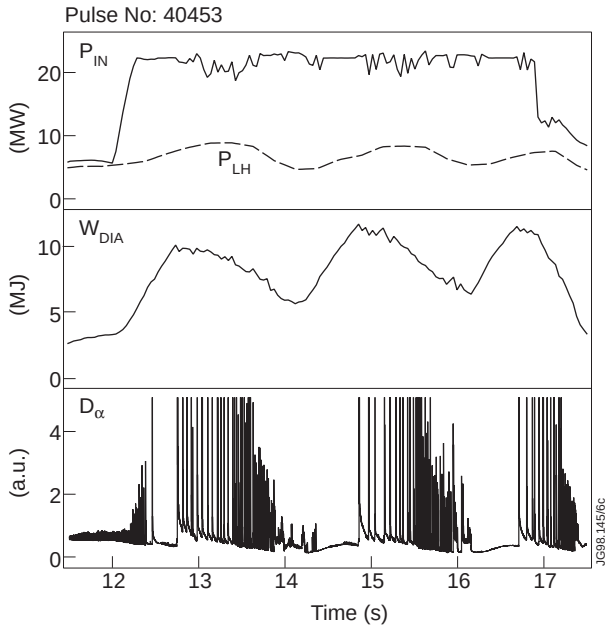

FIG. 22. Time traces of a 3.5MA discharge which undergoes two large losses of confinement from H-mode to L-mode levels.

At $I_P > 3.5$MA most discharges suffer from a spontaneous H-L "back-transition" (Fig. 22). The loss of confinement (sometimes after several energy confinement times) is often followed by a nondisruptive locked mode. In some cases the confinement recovers a few seconds after the loss; up to three cycles have been observed in pulses with long duration additional heating. The H-L transition tends to occur at a constant value of P/n_eB_T, i.e. at a fixed relationship to the L-H threshold. This is despite the fact that the loss of confinement occurs well above normal threshold power for the initial L-H transition. There is variation of this value from day to day, suggesting that vessel conditions may also be important. At 2.5MA, where normally H-modes can be maintained for all of the available heating length (up to 10 s), a similar H-L transition is seen in shots with reduced NB heating powers, in particular if the vacuum vessel is not very well conditioned.

4. SUMMARY AND IMPLICATIONS FOR ITER

A central issue for ITER is the degree to which the integrated performance of the plasma/edge/divertor can be influenced by choice of divertor geometry. A general summary of the changes seen in going from Mark I to Mark IIA and then reducing the bypass leaks (Mark IIAP) is as follows. Increasing closure has produced three expected effects: the density for the onset of detachment, for a given P_{sol}, was reduced; the pumping speed was increased (Mark I $\rightarrow$ Mark IIA); and the main chamber neutral pressure was reduced (Mark IIA $\rightarrow$ Mark IIAP). It had also been expected that the intrinsic impurity level of the core plasma would be reduced, which did not occur. The explanation seems to lie in the fact that (a) there is more direct ion impact on the divertor shoulders of the narrower Mark II, (b)the higher tile operating temperature of Mark II leads to increased chemical sputtering, and (c) the carbon cladding of the inner wall was increased. The pump-out time for injected trace neon was reduced considerably in going from Mark I to Mark IIA.

The influence of these observed changes on global confinement was generally small. The H-mode density limit appears to be unchanged, and to be close to but slightly below the Greenwald value. The L$\rightarrow$H threshold appears to be independent of divertor closure or target orientation, but more investigation is needed on this point.

For Type I ELMy H-mode operation, the ELM frequency has a stronger effect on performance than either target orientation or flux expansion, and the ELM frequency is determined (at a given power and density) primarily by triangularity and gas puff rate.

In going from Mark IIA to Mark IIAP, it was possible to separate the effects of neutral pressure in the divertor and the midplane. Experiments showed that

the confinement quality of ELMy H-modes was better correlated with divertor neutral pressure and with separatrix electron density than with midplane neutral pressure. It is thus unlikely that improved core confinement, relative to present day machines, will be obtained in ITER simply from reduced midplane neutral pressure.

In order to operate successfully, ITER requires an "integrated scenario" in which the density is at or above the Greenwald value, the confinement quality is good enough ($H97 \geq 1.0$), the impurity content is low enough ($Z_{eff} \leq 1.8$), and the helium exhaust is sufficient to remove ash ($\tau_{He^*}/\tau_E \leq 5$). In addition, the temperature of the divertor and first wall components must remain below melting/ablation temperatures at all times (even during transients such as ELMs) such that the erosion rate is low enough to ensure reasonable component lifetimes.

When ELMy H-modes are operated with hot, medium density edges, the confinement quality is good and follows gyro-Bohm scaling. In addition, the Z_{eff} resulting from intrinsic impurities is quite low and well within the ITER requirements. The Type I ELMs which occur in the neutral beam heated H-modes result in core energy losses in the range $\Delta W/W \approx 3\% - 8\%$ and characteristic energy deposition times of 100 μs. Such ELMs, when extrapolated to ITER, would result in unacceptable heating and erosion of the divertor target plates unless there were a significant increase of the power deposition area, either on the divertor or by interaction with other first wall components. This is the principal objection to this mode of operation. It must be said, however, that the basis for extrapolating ELM sizes and power deposition footprints to ITER is poor and that more work is needed on this subject.

The ELMs produced in comparable RF heated ELMy H-modes are much smaller in amplitude and higher in frequency than ELMs in NB heated discharges, while the global confinement remains very good. The edge confinement, as measured by the pressure at the top of the edge pedestal, is significantly smaller in the presence of these small ELMs. This leads us to conclude that large edge pedestals and good edge confinement are possible only in the presence of large, Type I ELMs. Since the good global confinement in RF shots is due to peaked power deposition and since the α heating in ITER is calculated to have a profile intermediate between JET RF and NB heated pulses, it is likely that operation in ITER with small ELMs in order to protect first wall components will also lead to confinement which is less than that predicted based on current scaling laws. Whether or not it is necessary to operate ITER with small ELMs will depend on the scaling of the energy deposition by large, Type I ELMs, and on the scaling of the density limit, which can perhaps be ameliorated by central fuelling. Both scalings have yet to be put on a sound basis, something which is a priority for future divertor experiments on JET.

REFERENCES

[1] ALTMANN, H. and ANDREW, P., Closure of the bypass leakage around the JET divertor with polymer seals, Technical report, JET Joint Undertaking, 1997, JET Report JET-P(97)42.

[2] MATTHEWS, G. F. et al., Nucl. Fusion **38** (1998) ????

[3] HILL, D. N., J. Nucl. Mater. **241-243** (1997) 182.

[4] ITER Confinement Database and Modelling Working Group (presented by J .G. Cordey, Plasma Physics and Controlled Fusion **39** (1997) B115.

[5] GREENWALD, M. et al., Nucl. Fusion **28** (1988) 2199.

[6] LOARTE, A. et al., Nucl. Fusion **38** (1998) 331.

[7] SIMONINI, R. et al., An interpretative/predictive study of JET mark II divertors for ELMy H-modes in JET, in *Controlled Fusion and Plasma Physics (Proc. 24th Eur. Conf. Berchtesgaden, 1997)*, volume 21A, p. 13, Geneva, 1997, European Physical Society, Part I.

[8] MCCRACKEN, G. M. et al., Nucl. Fusion **38** (1998) ????

[9] LACKNER, K., Comments on Plasma Physics and Controlled Fusion **15** (1994) 359.

[10] SAIBENE, G. et al., Steady state h-modes at high plasma density in JET, in *Controlled Fusion and Plasma Physics (Proc. 24th Eur. Conf. Berchtesgaden, 1997)*, volume 21A, p. 49, Geneva, 1997, European Physical Society, Part I.

[11] FISHPOOL, G. M., Loss of confinement due to reduction of the edge pedestal in JET, Technical report, JET Joint Undertaking, 1997, JET Report JET-P(97)30, to be published in Nucl. Fusion.

[12] KUPSCHUS, P. et al., Experiments on plasma fuelling and elm control by pellet injection on JET, in *Controlled Fusion and Plasma Physics (Proc. 24th Eur. Conf. Berchtesgaden, 1997)*, volume 21A, p. 45, Geneva, 1997, European Physical Society, Part I.

[13] KAUFMANN, M. et al., Overview of ASDEX upgrade results, in *Fusion Energy 1996 (Proc. 16th Int. Conf. Montréal, Canada, 1996)*, volume 1, p. 79, Vienna, 1997, IAEA.

[14] The JET Team (presented by M. Keilhacker), Plasma Physics and Controlled Fusion **39** (1997) B1.

[15] HORTON, L. D. et al., Plasma Physics and Con-

trolled Fusion **38** (1996) A269.

[16] GRUBER, O. et al., Plasma Physics and Controlled Fusion **39** (1997) B19.

[17] ITER Team, Technical basis for the ITER detailed design report, cost review and safety analysis (DDR), ITER EDA Documentation Series 13, IAEA, Vienna, 1997.

[18] RYTER, F. and H Mode Database Working Group, Nucl. Fusion **36** (1996) 1217.

[19] ITER Confinement Database and Modelling Expert Group (Presented by T. Takizuka), Threshold power and energy confinement for ITER, in *Fusion Energy 1996 (Proc. 16th Int. Conf. Montréal, Canada, 1996)*, volume 2, p. 795, Vienna, 1997, IAEA.

[20] The ITER H-mode Database Working Group (Presented by J. Snipes), An analysis of the H-mode threshold in ITER, in *Controlled Fusion and Plasma Physics (Proc. 24th Eur. Conf. Berchtesgaden, 1997)*, volume 21A, p. 961, Geneva, 1997, European Physical Society, Part III.

[21] WAGNER, F. et al., Recent results of H-mode studies on ASDEX, in *Plasma Physics and Controlled Nuclear Fusion Research 1990 (Proc. 13th Int. Conf. Washington, DC, 1990)*, volume 1, p. 277, Vienna, 1991, IAEA.

[22] The JET Team (Presented by J. G. Cordey), Energy confinement and H-mode power threshold scaling in JET with ITER dimensionless parameters, in *Fusion Energy 1996 (Proc. 16th Int. Conf. Montréal, Canada, 1996)*, volume 1, p. 603, Vienna, 1997, IAEA.

[23] ALTMANN, H. et al., Fusion Technology **1** (1994) 275.

[24] PACHER, H. D. et al., J. Nucl. Mater. **241-243** (1997) 255.

[25] H. D. Pacher, ITER design description document, ITER Report G 17 DDD 1 96-08-21, W2.1, IAEA, Vienna, 1996, Appendix E9, Section 1.7 (Divertor).

[26] MOHANTI, R. et al., Satistical analysis of type I ELMs at JET, in *Controlled Fusion and Plasma Physics (Proc. 24th Eur. Conf. Berchtesgaden, 1997)*, volume 21A, p. 101, Geneva, 1997, European Physical Society, Part I.

[27] GAUTHIER, E. et al., ELM dynamics and power deposition in the JET divertor, in *Controlled Fusion and Plasma Physics (Proc. 24th Eur. Conf. Berchtesgaden, 1997)*, volume 21A, p. 61, Geneva, 1997, European Physical Society, Part I.

[28] LINGERTAT, J. et al., The effects of ELMs on the plasma edge of JET, in *Controlled Fusion and Plasma Physics (Proc. 22nd Eur. Conf. Bournemouth, 1995)*, volume 19C, p. 281, Geneva, 1995, European Physical Society, Part III.

[29] LINGERTAT, J. et al., J. Nucl. Mater. **241-243** (1997) 402.

[30] SARTORI, R. et al., Confinement and performance of high current steady state ELMy H-modes with the JET mark II divertor, in *Controlled Fusion and Plasma Physics (Proc. 24th Eur. Conf. Berchtesgaden, 1997)*, volume 21A, p. 73, Geneva, 1997, European Physical Society, Part I.